

Performance of Coded DS-CDMA With Pilot-Assisted Channel Estimation and Linear Interference Suppression

Wayne G. Phoel, *Member, IEEE*, and Michael L. Honig, *Fellow, IEEE*

Abstract—We consider a direct sequence (DS-) code division multiple access (CDMA) system with orthogonally multiplexed pilot signals and minimum mean squared error (MMSE) data and channel estimation. Both flat and frequency-selective fading channels are considered. Large system analysis is used to optimize the pilot-to-data power ratio (PDR) and the code rate for a fixed bandwidth expansion. Specifically, the PDR is selected to minimize the probability of error subject to a constraint on transmitted power. When the MMSE filter estimates the channel of the desired user, but averages over the channels of the interferers (corresponding to an adaptive filter in moderate to fast fading), the optimal PDR is less than that for the matched filter (MF). That is, the MMSE filter benefits from allocating more power to the data. When the MMSE filter directly incorporates estimates of all users' channel coefficients, the optimal PDR is greater than that for the MF. System performance as a function of code rate is characterized through both probability of error and cutoff rate. The optimal code rate for the MMSE receiver is generally higher than that for the MF, and increases with load and E_b/N_0 . In the presence of fading, and with channel estimation, the optimal code rate approaches zero for both MMSE and MF receivers, but the MMSE filter is more robust with respect to a suboptimal choice of code rate.

Index Terms—Code division multiple access (CDMA), fading channels, minimum mean squared error (MMSE) estimation.

I. INTRODUCTION

WIDEBAND direct-sequence (DS-) code division multiple access (CDMA) with pilot-assisted coherent detection has been proposed as the basis for next generation cellular systems [1], [2]. In this paper, we study the coded performance of the linear minimum mean squared error (MMSE) receiver with pilot-assisted channel estimation, and compare it with the conventional matched filter (MF), or coherent RAKE receiver. Specifically, each user transmits a known pilot signal spread orthogonally to the data for the purpose of channel

estimation. Given a fixed transmitted power constraint, the system performance depends on how the power is split between the pilot and data signals. We also fix the bandwidth expansion and study the tradeoff between error control coding and random spreading.

Our analytical approach is to evaluate the large system error probability, in which the processing gain N and the number of users K approach infinity with fixed ratio K/N [3]. We extend prior analyses to evaluate system performance when orthogonally multiplexed pilot signals are used for channel estimation in the presence of multipath fading. Related work on the performance of the MMSE receiver in the presence of frequency-selective fading and with imperfect channel estimation has been presented in [4]. Our model differs from the one in [4] in that we include orthogonally multiplexed pilot signals. In addition, our focus is on single-user receivers which average over the channels of the interferers (see [5]). A comparison with simulation results shows that this analysis accurately predicts the performance of finite systems of interest.

Optimization of the pilot-to-data power ratio (PDR) has previously been studied for the MF receiver [6], [7]. When an MMSE filter incorporates a channel estimate for the desired user, but averages over the channels of the interferers, our results show that the optimal PDR is lower than that for the MF. The optimal PDR increases when the MMSE filter incorporates estimates for all interferers' channels.

Large system analysis is also used to study coded performance with channel estimation. The code rate is optimized with respect to both cutoff rate and the union bound on probability of error for some specific convolutional codes. Although the optimal code rate for the MMSE receiver is generally higher than that for the MF, both receivers benefit from low code rates in the presence of fading or with a small load (K/N). Our results also show that the MMSE receiver is robust with respect to the selection of a suboptimal code rate. Related work on the selection of code rate for the additive white Gaussian noise (AWGN) channel has been presented in [8] and [9]. The latter work is extended to Rayleigh fading in [10]. The effect of code rate on the performance of recursive least squares and MMSE filters in the presence of flat Rayleigh fading, with and without channel estimation, is considered in [11]. In [12]–[14], the code rate is optimized with respect to channel capacity for linear MMSE receivers. The effect of an independent pilot on the large system signal-to-interference-plus-noise ratio (SINR) is also discussed in [14].

Manuscript received September 25, 2000; revised October 1, 2001. This work was supported by a University Partnership in Research Grant from Motorola, Inc. and by the U.S. Army Research Office by Grant DAAD19-99-1-0288. This paper was presented in part at the Conference on Information Sciences and Systems (CISS), Johns Hopkins University, Baltimore, MD, March 1999, and IEEE Wireless Communications and Networking Conference (WCNC), Chicago, IL, September 2000.

W. G. Phoel was with the Department of Electrical and Computer Engineering, Northwestern University, Evanston, IL 60208 USA. He is now with MIT Lincoln Laboratory, Lexington, MA 02420 USA (e-mail: phoel@ll.mit.edu).

M. L. Honig is with the Department of Electrical and Computer Engineering, Northwestern University, Evanston, IL 60208 USA (e-mail: mh@ece.nwu.edu).

Publisher Item Identifier S 0090-6778(02)05110-3.

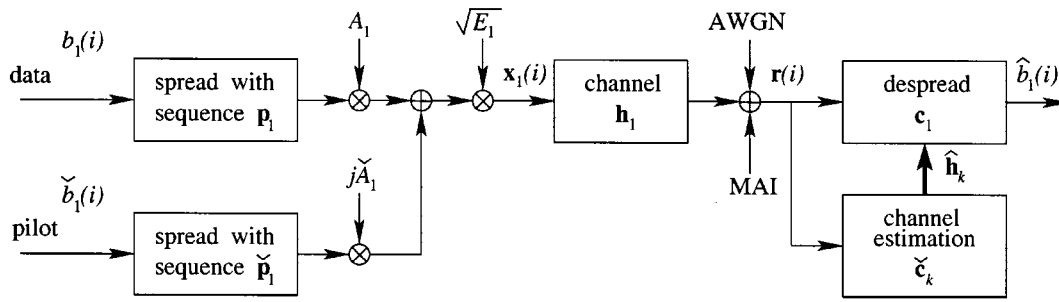


Fig. 1. System block diagram.

In Section II we present the DS-CDMA system model along with the data and channel estimation filters. Section III briefly reviews the large system results needed and discusses the necessary modifications which account for orthogonally multiplexed pilot signals, frequency-selective fading, and channel estimation spanning multiple symbol periods. Optimization of the PDR is presented in Section IV, and the selection of code rate is discussed in Section V.

II. SYSTEM MODEL

We consider the reverse link of an isolated DS-CDMA cell. Fig. 1 shows a block diagram of the system model for a single user. Each signal contains a pilot sequence spread orthogonally to the data to enable coherent detection. The signals experience frequency-selective Rayleigh fading and are corrupted by AWGN and multiple access interference (MAI).

The system is assumed to be synchronous with K users, each with processing gain N . Let the $(N \times 1)$ vector \mathbf{p}_k represent the spreading sequence of user k and let $b_k(i)$ denote the corresponding transmitted data symbol at time i . The pilot signal spreading sequence and symbol are denoted by $\check{\mathbf{p}}_k$ and $\check{b}_k(i)$, respectively. The baseband signal transmitted by user k at time i is

$$\mathbf{x}_k(i) = A_k \mathbf{p}_k b_k(i) + j \check{A}_k \check{\mathbf{p}}_k \check{b}_k(i) \quad (1)$$

where A_k and \check{A}_k are the amplitudes of the data and pilot signals, respectively. All error probability calculations assume binary signaling, so that $b_k(i), \check{b}_k(i) \in \{\pm 1\}$.

The PDR for user k is defined as $\beta_k = \check{A}_k^2 / A_k^2$, where we assume the normalization $A_k^2 + \check{A}_k^2 = 1$. The elements of \mathbf{p}_k are chosen with equal probability from the set $\{\pm \sqrt{1/2N} \pm j\sqrt{1/2N}\}$. To ensure that $\mathbf{p}_k^\dagger \check{\mathbf{p}}_k = 0$, where \dagger denotes complex conjugate transpose, the n th element of $\check{\mathbf{p}}_k$ is defined as

$$\check{p}_{k,n} \equiv \begin{cases} p_{k,n}, & \text{for } n \leq \frac{N}{2} \\ -p_{k,n}, & \text{for } n > \frac{N}{2} \end{cases} \quad (2)$$

and we constrain N to be even.

We assume a symbol-synchronous system with L shifted multipath components to simplify our analysis. (The large system analysis used here is extended to asynchronous CDMA in [15].) The delays of the primary paths are therefore zero for

all users. We assume that each subsequent path is delayed by exactly one chip period. The received vector for symbol i is given by

$$\mathbf{r}(i) = \sum_{k=1}^K \sum_{l=1}^L \sqrt{E_k} h_{k,l}(i) \mathbf{x}_k^{(l)}(i) + \mathbf{z}(i) + \boldsymbol{\xi}(i) \quad (3)$$

where E_k is the mean received energy per symbol for user k summed over all paths and includes both pilot and data signals, $h_{k,l}(i)$ is the channel coefficient associated with path l for user k , $\mathbf{z}(i)$ is a vector of complex-valued white Gaussian noise samples with variance $\sigma^2 = N_0/2$ per dimension, and $\boldsymbol{\xi}(i)$ is the intersymbol interference due to multipath. The vector $\mathbf{x}_k^{(l)}(i)$ has length $N + L - 1$, and contains the elements of $\mathbf{x}_k(i)$ given by (1) in positions l through $N + l - 1$, and zeros elsewhere.

The received vector $\mathbf{r}(i)$ contains the contributions from all paths for symbol i , and therefore has length $N + L - 1$. Consequently, the first $L - 1$ elements of $\mathbf{r}(i)$ are the same as the last $L - 1$ elements of $\mathbf{r}(i - 1)$. The vector $\boldsymbol{\xi}(i)$ accounts for the contributions from the data and pilot symbols at times $i - 1$ and $i + 1$. Therefore, the first and last $L - 1$ elements of $\boldsymbol{\xi}(i)$ are the only nonzero entries. Since we assume a fixed delay spread, for the subsequent large system analysis, the intersymbol interference is negligible as $N \rightarrow \infty$. Although we neglect intersymbol interference in our analysis, it is included in the simulation results presented in later sections.

The channel coefficients, $h_{k,l}(i)$, are modeled as independent, zero-mean, complex-valued, and circularly symmetric Gaussian random variables with variance $1/L$. For the simulation results in Sections IV and V, each channel coefficient varies in time according to a Gaussian random process with power spectrum $S(f) \propto (1/2\pi) \sqrt{1/(f_D^2 - f^2)}$ for $|f| < f_D$, where f_D is the maximum Doppler frequency. We assume each fading process is constant over one symbol period, but varies from symbol to symbol.

A. Data Estimation

We use a linear filter to estimate the signal sent by user 1. The soft symbol estimate is given by

$$\check{b}_1(i) = \mathbf{c}^\dagger \mathbf{r}(i) \quad (4)$$

where \mathbf{c} is either the MF or MMSE filter. The MF is the *effective* spreading sequence of the desired user; namely, the super-

position of the faded and delayed versions of the desired user's spreading sequence

$$\mathbf{c}_{mf} = \bar{\mathbf{p}}_1 \equiv \sum_{l=1}^L \mathbf{p}_1^{(l)} h_{1,l} \quad (5)$$

where $\mathbf{p}_1^{(l)}$ contains the spreading sequence for user 1 in chips l through $N + l - 1$ and the dependence on i is omitted for convenience.

The MMSE filter is chosen to minimize the cost function

$$\varepsilon = \mathbb{E}[|\tilde{b}_1 - b_1|^2] \quad (6)$$

where the expectation is with respect to the data symbols, pilot symbols, noise samples, and the channels of the interferers if they are not directly estimated. The optimal filter is

$$\mathbf{c}_{mmse} = A_1 \sqrt{E_1} \mathbf{R}^{-1} \bar{\mathbf{p}}_1 \quad (7)$$

where $\mathbf{R} = \mathbb{E}[\mathbf{r}\mathbf{r}^\dagger]$ is the covariance matrix of the received signal.

B. Channel Estimation

Both the MF and MMSE data estimation filters require estimates of the channel for the desired user. Furthermore, the MMSE filter performance can be improved by including estimates of the interferers' channels. We estimate the channel coefficient for each path separately, assuming perfect knowledge of the path delays, and then combine the shifted spreading sequences to estimate $\bar{\mathbf{p}}_1$.

Analogous to the data estimation, either an MF or MMSE filter can be used to estimate the channel. The channel estimation filter spans $TN + L - 1$ chips, requiring T stacked received vectors

$$\mathbf{r}_T(i) = [\mathbf{r}_{[1, N]}^\dagger(i), \mathbf{r}_{[1, N]}^\dagger(i-1), \dots, \mathbf{r}_{[1, N]}^\dagger(i-T+1)]^\dagger \quad (8)$$

where TN is less than the coherence time of the channel, the subscript $[1, N]$ indicates that we use only elements 1 through N of each $\mathbf{r}(\cdot)$, and the last vector in the stack contains all $N + L - 1$ elements. The estimate for the channel coefficient $h_{k,l}(i)$ is

$$\hat{h}_{k,l}(i) = (\check{\mathbf{c}}_k^{(l)})^\dagger \mathbf{r}_T(i) \quad (9)$$

where $\check{\mathbf{c}}_k^{(l)}$ is the appropriate filter, $\check{\mathbf{c}}_k$ (MF or MMSE), shifted by $l - 1$ chips.

The MF for user k is obtained by stacking the pilot signal spreading sequence, i.e.,

$$\check{\mathbf{c}}_{k,mf} = j [\check{b}_k(i)\check{\mathbf{p}}_k', \check{b}_k(i-1)\check{\mathbf{p}}_k', \dots, \check{b}_k(i-T+1)\check{\mathbf{p}}_k']' \quad (10)$$

where $'$ denotes transpose. The MMSE filter coefficients are chosen to minimize

$$\check{\varepsilon}_{k,l} = \mathbb{E} \left[\left| (\check{\mathbf{c}}_{k,mmse}^{(l)})^\dagger \mathbf{r}_T - h_{k,l} \right|^2 \right] \quad (11)$$

and take a form similar to (7)

$$\check{\mathbf{c}}_{k,mmse}^{(l)} = \check{A}_k \sqrt{E_k} \mathbf{R}_T^{-1} \check{\mathbf{c}}_{k,mf}^{(l)} \quad (12)$$

where $\mathbf{R}_T = \mathbb{E}[\mathbf{r}_T \mathbf{r}_T^\dagger]$ and again the expectation is with respect to the transmitted symbols, noise, and interferers' channels if they are not explicitly estimated.

III. LARGE SYSTEM ANALYSIS

For the CDMA model presented in Section II, the SINR at the output of the MMSE data estimation filter corresponding to user 1 is

$$\gamma_{mmse} = A_1^2 E_1 \bar{\mathbf{p}}_1^\dagger \mathbf{R}_{1-}^{-1} \bar{\mathbf{p}}_1 = \frac{E_1}{1 + \beta_1} \bar{\mathbf{p}}_1^\dagger \mathbf{R}_{1-}^{-1} \bar{\mathbf{p}}_1 \quad (13)$$

where \mathbf{R}_{1-} is the interference-plus-noise covariance matrix. In the absence of orthogonal pilot signals and multipath, $\mathbf{R}_{1-} = \mathbf{P}_{1-} \mathbf{D}_{1-} \mathbf{P}_{1-}^\dagger + 2\sigma^2 \mathbf{I}$, where \mathbf{P}_{1-} is the matrix whose columns are the signatures of the interferers and \mathbf{D}_{1-} is a diagonal matrix containing the energy of the interferers received in a symbol period. It is shown in [3] that for this case, as $N, K \rightarrow \infty$ and $K/N \rightarrow \alpha$, γ_{mmse} converges in probability to the deterministic limit

$$\gamma_{mmse}^* = \frac{E_1}{1 + \beta_1} \cdot \left[2\sigma^2 + \alpha \int \frac{E_1 \lambda}{E_1 + (1 + \beta_1) \lambda \gamma_{mmse}^*} dF_I(\lambda) \right]^{-1} \quad (14)$$

and the MF SINR, γ_{mf} , converges to

$$\gamma_{mf}^* = \frac{E_1}{1 + \beta_1} \left[2\sigma^2 + \alpha \int \lambda dF_I(\lambda) \right]^{-1} \quad (15)$$

where $F_I(\cdot)$ is the large system limit of the interference energy distribution.

The former result (14) relies on the large system limit of the distribution of eigenvalues of the interference covariance matrix, $\mathbf{R}_I = \mathbf{P}_{1-} \mathbf{D}_{1-} \mathbf{P}_{1-}^\dagger$, and requires the elements of \mathbf{P}_{1-} to be zero-mean i.i.d. random variables [16]. Each integral term in (14) and (15) is called the *effective interference* for the associated receiver. In the following sections, we modify the preceding expressions to account first for orthogonally multiplexed pilots, then separately for multipath, and finally combine the results.

A. Orthogonally Multiplexed Pilot Signals

Here we assume that all users have the same PDR, $\beta = \check{A}_k^2 / A_k^2$. When the pilot channel is included in the signal model, the pilot and data spreading sequences belonging to a given user are not independent so that the results of [3] cannot be directly applied. However, in the appendix we show that, because the pilot is spread orthogonally to the data, the effect of the pilot on the large system output SINR is the same as if it were spread with an independent random sequence. Our system with K users therefore becomes, effectively, a system with $2K$ users where half of the users (corresponding to the data) have power scaled by $1/(1 + \beta)$ and the other half (corresponding to the pilot)

have power scaled by $\beta/(1+\beta)$. Consequently, the large system SINR at the output of the MMSE data estimation filter is

$$\gamma_{mmse}^* = \frac{E_1}{1+\beta} \left[2\sigma^2 + \alpha \int \frac{E_1 \lambda}{(1+\beta)(E_1 + \lambda \gamma_{mmse}^*)} + \frac{E_1 \beta \lambda}{(1+\beta)(E_1 + \beta \lambda \gamma_{mmse}^*)} dF_I(\lambda) \right]^{-1}. \quad (16)$$

The SINR at the output of the MF remains the same as (15). This expression also appears in [14], where the elements of the pilot and data spreading sequences are assumed to be independent and circularly symmetric random variables. In that case, (16) follows as a direct extension of the results in [3].

B. Multipath

In the presence of multipath, the output SINR depends on how the receiver treats the time-varying interference. In [4], the receiver is assumed to estimate the channel for each user given knowledge of the path delays. The channel estimate for path l of user k is given by $h_{k,l} + \nu_{k,l}$ where $\nu_{k,l}$ is assumed to be Gaussian with variance ζ_k^2 . The large system SINR per path at the output of the MMSE filter (averaged over the fade of the desired user and ignoring the pilot signals for the moment) is then

$$\gamma_{mmse}^* = \frac{E_1}{L} \left[2\sigma^2 + \alpha \int \frac{E_1 \lambda}{E_1 + L \lambda \gamma_{mmse}^*} dH(\lambda) \right]^{-1} \quad (17)$$

where $H(\cdot)$ is the distribution function of the *estimated* interference energy. That is, there is interference from the effective spreading sequence of user k with energy $E_k(\sum_{l=1}^L |h_{k,l}|^2 + \zeta_k^2)$ and there is also interference from $L-1$ “virtual” interferers each with energy $E_k \zeta_k^2$ due to the estimation error associated with the separate multipath components. With perfect channel estimates, $\zeta_k^2 = 0 \forall k$ and $H(\cdot)$ depends only on the distribution of the amplitudes of the channel coefficients [10].

Now consider an adaptive filter which attempts to estimate the MMSE filter. Motivated by the approach in [5], we assume that the adaptive filter averages over the channels of the interferers. That is, each path is treated as an independent interferer subject to flat fading. In forming \mathbf{R} , we take the expected value over the channel coefficients, resulting in

$$\mathbf{R} = \sum_{l=1}^L \mathbf{P}^{(l)} \mathbf{D} \mathbf{P}^{(l)\dagger} + 2\sigma^2 \mathbf{I} \quad (18)$$

where $\mathbf{P}^{(l)}$ is \mathbf{P} shifted by $l-1$ chips. The elements of $\mathbf{P}^{(l_1)}$ are correlated with those of $\mathbf{P}^{(l_2)}$ for all l_1, l_2 so that the assumptions used to derive (14) do not apply. However, since the channel coefficients are independent across paths, as an approximation, we treat the columns as independent. We therefore approximate the SINR per path as in (14) with α replaced by $L\alpha$ and λ scaled by $1/L$

$$\gamma_{mmse}^* \approx E_1 \left[2L\sigma^2 + L\alpha \int \frac{E_1 \lambda}{E_1 + \lambda \gamma_{mmse}^*} dF_I(\lambda) \right]^{-1}. \quad (19)$$

The simulation results in Section IV show that this approximation is accurate. The approximation is exact for circularly-symmetric spreading sequences [4]. For the MF, the large system SINR is again given by (15).

Combining the effects of multipath and pilot signals, we obtain the following expressions. If the receiver estimates the channels for all users, then for the pilot-assisted scheme considered, the large system SINR per path at the output of the MMSE data estimation filter is

$$\gamma_{mmse}^* \approx \frac{E_1/L}{1+\beta} \left[2\sigma^2 + \alpha \int \left(\frac{E_1 \lambda}{(1+\beta)(E_1 + L \lambda \gamma_{mmse}^*)} + \frac{E_1 \beta \lambda}{(1+\beta)(E_1 + L \beta \lambda \gamma_{mmse}^*)} \right) dH(\lambda) \right]^{-1} \quad (20)$$

where the variance of the channel estimates, ζ^2 , is determined from the channel estimation filter output SINR described in Section III-C. If the receiver averages over the channels of the interferers, then

$$\gamma_{mmse}^* \approx \frac{E_1}{1+\beta} \left[2L\sigma^2 + L\alpha \int \left(\frac{E_1 \lambda}{(1+\beta)(E_1 + \lambda \gamma_{mmse}^*)} + \frac{E_1 \beta \lambda}{(1+\beta)(E_1 + \beta \lambda \gamma_{mmse}^*)} \right) dF_I(\lambda) \right]^{-1} \quad (21)$$

where we assume L -path fading for all users.

C. Channel Estimation

The derivation of the large system output SINR for the channel estimation filter is analogous to that for the data estimation filter. The channel estimation filter has length NT , but each interferer transmits two sets of T different symbols within this time span, corresponding to the pilot and data signals. (In contrast to the analysis in [4], we assume no knowledge of the interferers’ data symbols.) The SINR associated with the MMSE channel estimate is

$$\tilde{\gamma}_{mmse} = \frac{\beta E_k}{1+\beta} \left(\hat{\mathbf{c}}_{k,mf}^{(t)} \right)^\dagger \mathbf{R}_T^{-1} \hat{\mathbf{c}}_{k,mf}^{(t)}. \quad (22)$$

As $K, N \rightarrow \infty$ and $K/N \rightarrow \alpha$, it is shown in the appendix that the SINR for the MMSE channel estimate converges in probability to

$$\begin{aligned} \tilde{\gamma}_{mmse}^* &\approx \frac{\beta T E_k / L}{1+\beta} \\ &\cdot \left[2\sigma^2 + \alpha \int \frac{\beta T E_k \lambda / L}{\beta T E_k / L + (1+\beta) \lambda \tilde{\gamma}_{mmse}^*} dF_{I_2}(\lambda) \right]^{-1} \\ &= \beta T \gamma_{mmse}^* \end{aligned} \quad (23)$$

where $F_{I_2}(\cdot)$ is the distribution function of the interference, treating the pilot and data signals as separate users, and the channel estimation filter is assumed to average over the channels and symbols of the interferers. That is, the interference can be viewed as originating from T “virtual” users, each having spreading sequence length equal to the length of the channel

estimation filter, and each transmitting at $1/T$ times the interferer's power. The large system SINR associated with the channel estimate for user k is then given by (21) with E_1 replaced by βTE_k .

IV. OPTIMIZATION OF PILOT-TO-DATA RATIO (PDR)

We now use the preceding results to optimize the PDR β . Our approach is analogous to that taken in [6] for the MF. In what follows we will assume that the interference-plus-noise at the output of the despreading filter (either MMSE or MF) is Gaussian. This approximation is examined in [17] for the linear MMSE receiver and is shown to be accurate in cases of interest. Furthermore, for the synchronous AWGN channel this approximation becomes exact as $K, N \rightarrow \infty$. The (uncoded) probability of error with channel estimates is then

$$P_e = \frac{1}{2} \left[1 - \mu \sum_{l=0}^{L-1} \binom{2l}{l} \left(\frac{1-\mu^2}{4} \right)^l \right] \quad (24)$$

where

$$\mu = \left[\left(1 + \frac{1}{\gamma} \right) \left(1 + \frac{1}{\tilde{\gamma}} \right) \right]^{-1/2} \quad (25)$$

and γ and $\tilde{\gamma}$ are the mean SINR's per path (averaged over the desired user's channel) for the data and pilot signals, respectively (see [18, Appendix B]). Minimizing P_e is equivalent to maximizing μ . From (25) it is clear that both γ and $\tilde{\gamma}$ must be large for good performance. We remark that for the MMSE receiver (16), the effective interference depends on β whereas for the MF receiver (15), β affects only the desired signal power.

We also consider the effect of the PDR on coded bit error rate (BER). The union bound on BER for a rate k/n convolutional code can be written as

$$P_b \leq \frac{1}{k} \sum_{d=1}^{\infty} a_d P_e(d) \quad (26)$$

where $P_e(d)$ is the pairwise error probability of choosing a path of weight d over the all-zero path, and a_d is the total number of nonzero information bits corresponding to all error paths with Hamming weight d . With pilot-assisted channel estimation and independent fading, $P_e(d)$ can be calculated from (24) by replacing L with Ld . Since μ does not depend on d , the β that maximizes μ also minimizes the bound on P_b .

As an example of the effect of PDR on system performance, Fig. 2 compares the bit error rate based on the large system SINR with simulation results for both MF and MMSE receivers for $\alpha = 0.25$, $L = 3$ and $E_k/N_0 = 7$ dB. Curves labeled MMSE correspond to MMSE estimation of both data and channels. Similarly, results for the MF assume that both the data and the channels are estimated with an MF. Each channel is estimated over $T = 10$ symbol periods as described in Section II. Results are shown for a rate $1/2$ convolutional code with octal generator matrix (345, 237). The simulation results correspond to a processing gain of $N = 128$ and a block length of 1000 bits, which enables effective interleaving at the simulated fade rate ($f_D T_s = 0.0093$ where T_s is the symbol period).

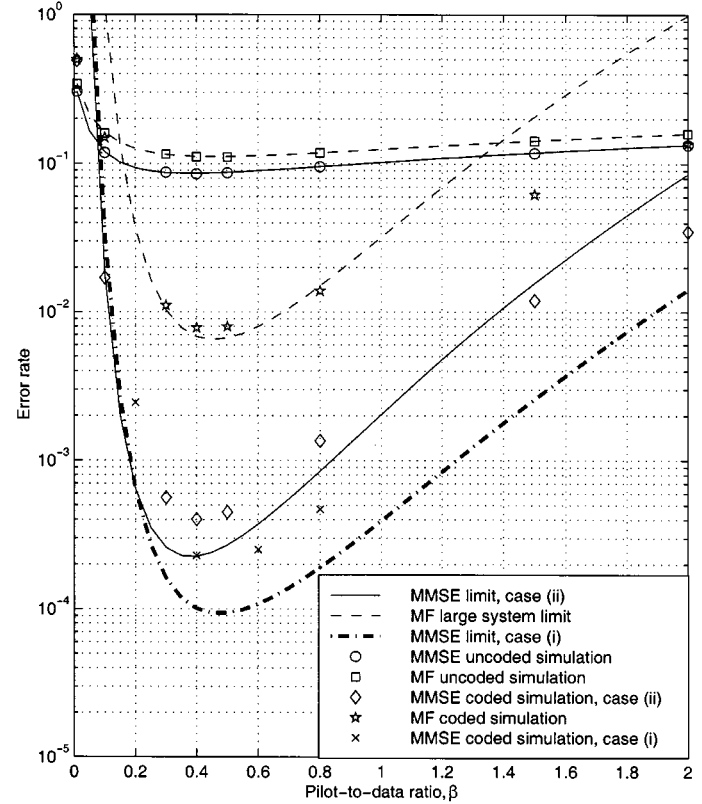


Fig. 2. Bit error rate versus PDR with $\alpha = 0.25$, $L = 3$, and $E_k/N_0 = 7$ dB.

Results are shown for the two cases discussed: i) The MMSE filter incorporates channel estimates for all users, and ii) The MMSE filter averages over the channels of the interferers. The optimal PDR for case i) is somewhat larger than that for case ii), reflecting the greater dependence on channel estimates for interference suppression. The performance improvement associated with case i) relative to case ii) is not as large as might be expected due to the virtual interference associated with the inaccurate channel estimates. The simulation results at low BER (i.e., approximately 10^{-3} and below) are greater than the analytical results based on the upper bound (26) because the analytical results assume perfect interleaving and are exact only as $N \rightarrow \infty$. Still, the general shape of the simulated results match the shape of the analytical curves.

Fig. 3 shows the optimal PDR over a range of loads for $E_k/N_0 = 7$ dB and number of paths $L = 1$ and 3. These results, based on the large system analysis and computed numerically, assume $T = 10$ and correspond to the preceding case ii). The optimal PDR for the MMSE receiver is consistently less than that for the MF. The difference between the MMSE and MF curves is smaller for $L = 3$ than for $L = 1$. This is because increasing L increases the effective load for the MMSE receiver, but not for the MF receiver. As $\alpha \rightarrow 0$, and as $\alpha \rightarrow \infty$, the MMSE SINR converges to the MF SINR, so that the optimal PDR's for the two receivers converge to the same limit. A longer channel estimation filter (larger T) will result in a lower optimal PDR, provided NT is less than the coherence time of the channel. For example, the channel estimation filter used in [7] corresponds to $T = 16$ and the optimal $\beta \approx 0.3$ for

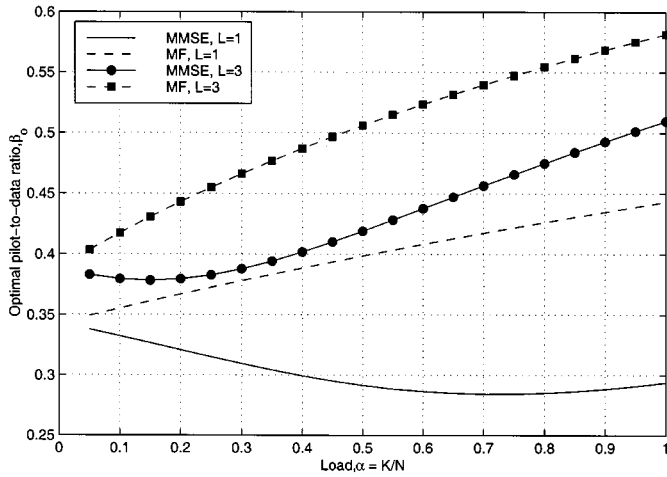


Fig. 3. Optimal PDR, β_o , as a function of load for $L = 1$ and 3 paths [case ii)], $E_k/N_0 = 7$ dB, and $T = 10$.

$L = 3$. This indicates that the optimal PDR generally increases with fade rate.

V. OPTIMIZATION OF CODE RATE

As in previous work [9], we fix the bandwidth expansion (chip rate / information rate) and analyze the tradeoff between random spreading and error control coding. For the MF, it is known that the code rate r should be small [19]. Generally, the optimal code rate for the MMSE receiver should be higher, since a larger number of random chips per coded symbol, N , provides more degrees of freedom for interference suppression. We use the expressions for the large system SINR to study this tradeoff, noting that the residual interference-plus-noise at the output of the despreading filter is Gaussian in the large system limit [20]. Whereas others have considered the capacity as a performance measure [21], [12], [13], here we study the cutoff rate, R_0 , and the union bound on the bit error probability.

In what follows, we will refer to the following cases:

- 1) *AWGN channel with perfect power control.* In this case $F_T(\lambda)$ is a step function at $\lambda = E_1$ (assuming $\beta = 0$) and the fixed point SINR equation can be solved as a quadratic. We remark that this situation also applies to flat fading channels with perfect channel estimation and perfect power control.
- 2) *Multipath with moderate fade rate, no power control.* In this case we assume that the fading is slow enough so that the channel of the desired user can be tracked, but it is too fast to allow an adaptive filter to track the channels of the interferers.

We first assume perfect knowledge of the desired user's channel and subsequently present results which include the effects of channel estimation.

A. Cutoff Rate

For the single-user AWGN channel, the cutoff rate is given by [18]

$$R_0 = 1 - \log_2(1 + e^{-E_s/N_0}) \quad (27)$$

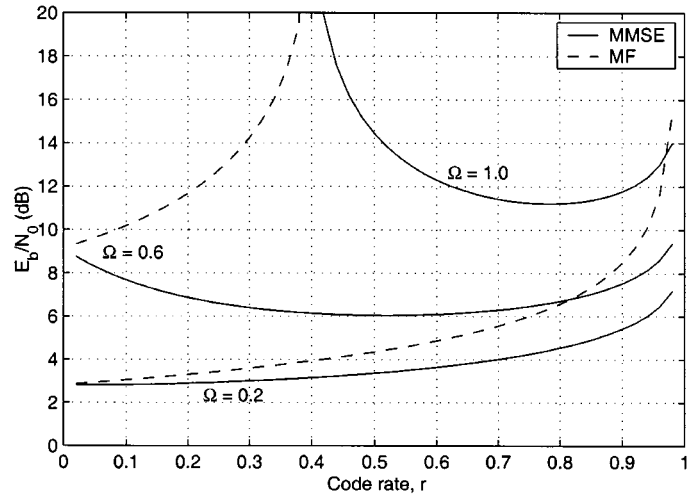


Fig. 4. Cutoff rate versus E_b/N_0 for fading channel, perfect power control (Case 1).

where $E_s = E_b r$. For a given E_b/N_0 , R_0 is found by setting $r = R_0$ and solving the fixed-point equation. For a power-controlled CDMA system with AWGN (Case 1), the large system E_s/N_0 at the input to the decoder is γ^* given by (14) and (15) for the MMSE and MF filters, respectively. The cutoff rate for a large system ($K, N \rightarrow \infty$ and $K/N \rightarrow \alpha$) is therefore

$$R_0 = 1 - \log_2(1 + e^{-\gamma^*}) \quad (28)$$

where γ^* is a function of α, r and E_b/N_0 .

Fig. 4 shows the corresponding E_b/N_0 versus code rate $r = R_0$ for different loads, $\Omega = \alpha r$. That is, Ω is the ratio of users, K , to the bandwidth expansion, N/r . We assume all users have the same E_b/N_0 . The optimal R_0 for a given load is the rate at which the corresponding curve in Fig. 4 is minimized. Note that the optimal rate for the MMSE receiver increases with load. The curves are generally shallow, which implies that performance is insensitive to the selection of code rate in the vicinity of the optimal value. From this figure we see that the optimal code rate for the MMSE filter at a load of 0.6 is approximately $r = 1/2$. As expected, the optimal rate for the MF approaches zero. Furthermore, the MMSE filter can support a load of $\Omega = 1$, given sufficient E_b/N_0 , whereas the MF cannot.

In the presence of fading, the Chernoff bound can be applied to the pairwise error probability [18], giving

$$R_0 = 1 - \log_2 \left[1 + \left(\frac{1}{1 + \gamma^*} \right)^L \right]. \quad (29)$$

Fig. 5 illustrates the relationships among R_0, α and E_b/N_0 for a frequency-selective Rayleigh fading channel with $L = 3$ independent paths and ideal interleaving (Case 2). The optimal code rate appears to approach zero for both receivers. Moreover, as the code rate approaches the optimal value, both the MMSE and MF receivers require the same E_b/N_0 , although the MMSE receiver is more robust with respect to a suboptimal code rate. Of course, this set of results depends on the assumption that the MMSE filter is unable to track the channels of the interferers.

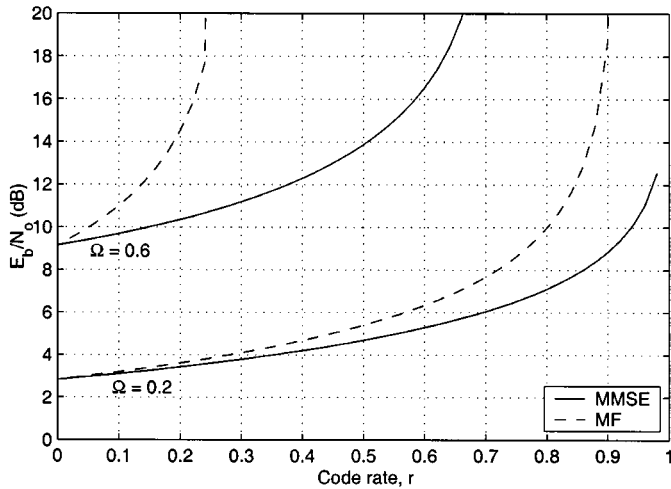


Fig. 5. Cutoff rate versus E_b/N_0 with frequency-selective fading (Case 2, $L = 3$) and no power control. The MMSE filter averages over the channels of interferers.

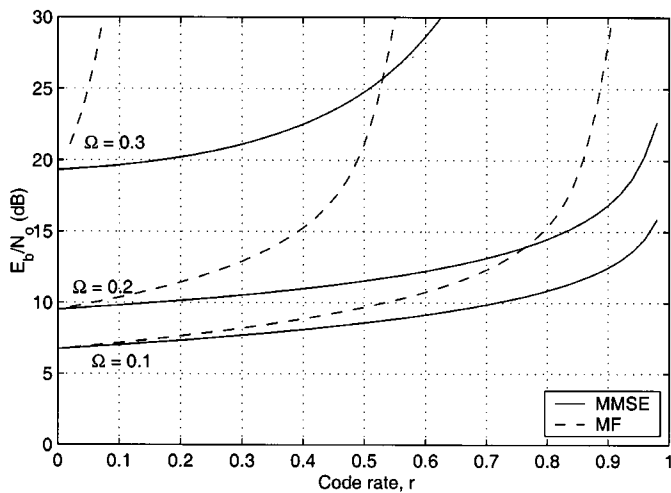


Fig. 6. Cutoff rate versus E_b/N_0 with frequency-selective fading (Case 2, $L = 3$), no power control, and pilot-assisted channel estimation. The MMSE filter averages over the channels of interferers.

Also, note that the additional E_b/N_0 needed for reliable communications in Rayleigh fading, relative to the AWGN channel, increases with load.

With the addition of the pilot channel, the cutoff rate has been shown to be [7]

$$R_0 = 1 - \log_2 \left[1 + \left(1 + \frac{\gamma^* \tilde{\gamma}^*}{1 + \gamma^* + \tilde{\gamma}^*} \right)^{-L} \right] \quad (30)$$

which can be rearranged as

$$R_0 = 1 - \log_2 \left[1 + (1 - \mu^2)^L \right] \quad (31)$$

where μ is given in (25). We wish to select the PDR to maximize μ . That is, maximizing μ maximizes R_0 for a given load and E_s/N_0 . Fig. 6 illustrates the relationships among R_0 , α and E_b/N_0 for a frequency-selective Rayleigh fading channel with $L = 3$ independent paths and pilot-assisted channel estimation where the PDR is optimized for each set of parameters. The MMSE filter averages over the channels of the interferers and

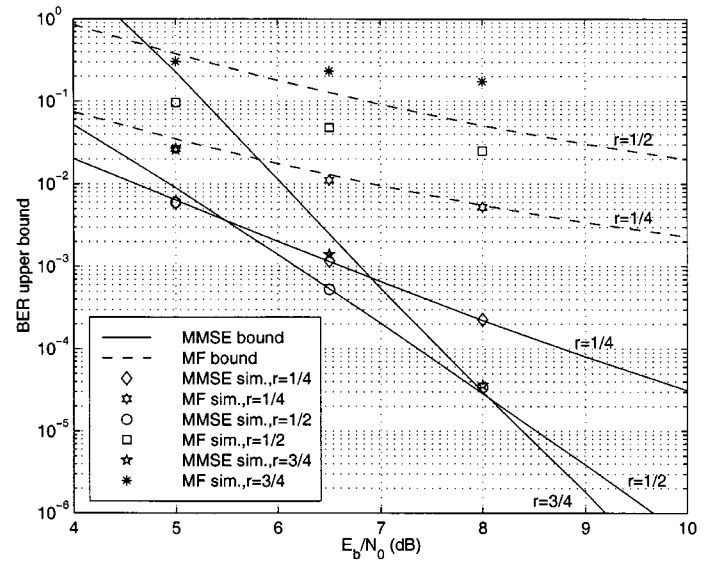


Fig. 7. Union bound on BER with perfect power control (Case 1) for code rates $r = 1/4, 1/2, 3/4$ and normalized load $\Omega = 0.6$.

the channel estimation filter has length corresponding to $rT = 5$ symbols. Comparing these results with those in Fig. 5 shows that channel uncertainty significantly decreases the supportable load. Still, the MMSE filter is robust with respect to the choice of a suboptimal code rate.

B. Probability of Error

Here we assume specific convolutional codes and compute the upper bound on BER given by (26). We first assume perfect channel estimates and then present results with pilot-assisted channel estimation. For the AWGN channel, we assume that the interference plus noise is Gaussian so that $P_e(d) = Q(\sqrt{d\gamma})$ where γ is the output SINR of the despreading filter.

For the Rayleigh fading channel, we assume that the channel coefficients are independent from symbol to symbol (ideal interleaving) and across paths. (This also applies to the simulation results.) In addition, we assume equal mean gains for all paths. It follows that $P_e(d)$ is the probability of error with diversity order Ld and coherent combining given by

$$P_e(d) = \left[\frac{1}{2} (1 - \theta) \right]^{Ld} \sum_{l=0}^{Ld-1} \binom{Ld-1+l}{l} \left[\frac{1}{2} (1 + \theta) \right]^l \quad (32)$$

where $\theta = \sqrt{\gamma/(1 + \gamma)}$ and γ is the mean SINR per path at the filter output [18].

Fig. 7 compares the large system BER bound as a function of E_b/N_0 for Case 1 with code rates 1/4, 1/2 and 3/4, and load $\Omega = Kr/N = 0.6$. Numerical results for $N = 100$ are also shown. The rate 1/4 and 1/2 codes have generator matrices (353, 335, 277, 231) and (345, 237), respectively. The rate 3/4 code is a punctured convolutional code derived from the rate 1/2 code using puncturing pattern (1,1,1,0,0,1). For the MMSE filter, and for the range of error rates of interest (between 10^{-6} and 10^{-3}), the rate 1/2 and 3/4 codes perform best and exhibit similar performance. This is consistent with the cutoff rate results in Fig. 4. Also, as expected, the performance of the MF improves as the code rate decreases.

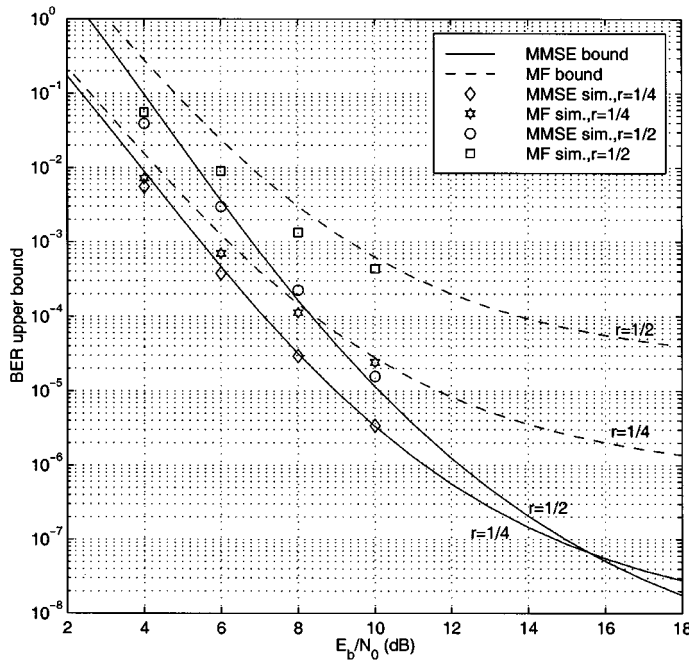


Fig. 8. Union bounds on BER with frequency-selective fading and no power control (Case 2, $L = 3$) for code rates $r = 1/2, 1/4$ and load $\Omega = 0.35$. The MMSE filter averages over the interferers' channels.

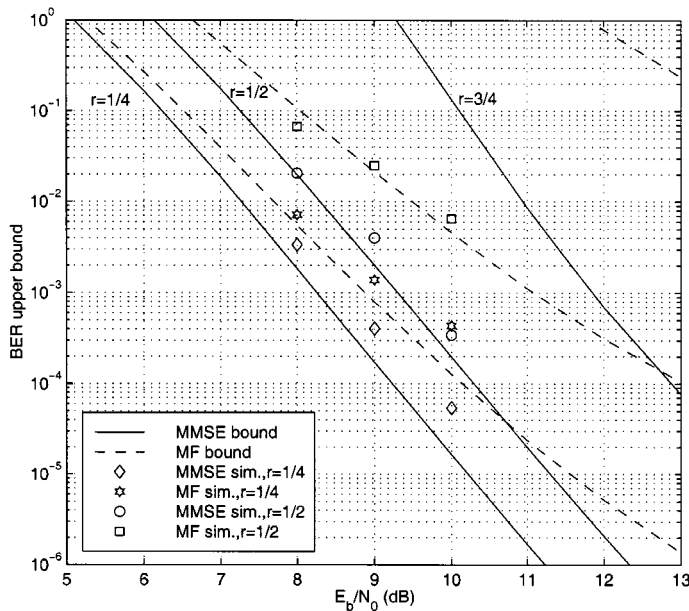


Fig. 9. Union bounds on BER with frequency-selective fading ($L = 3$), pilot-assisted channel estimation, and no power control. The load $\Omega = 0.125$, and the MMSE filter averages over the interferers' channels.

A similar comparison, corresponding to Case 2 with $L = 3$, is shown in Fig. 8 for $\Omega = 0.35$ ($N = 100$ for the simulation results). This plot shows that the rate 1/4 code is best for $E_b/N_0 < 16$ dB but that the rate 1/2 code is the best for larger E_b/N_0 (corresponding to very low P_e). As expected, the rate 1/4 code performs best for the MF.

Our final comparison accounts for inexact channel estimates based on the discussion of PDR in Section IV. Fig. 9 compares the performance of the convolutional codes used to generate the preceding plots. For these results, the load $\Omega = 0.125$,

which corresponds to the scenario considered in Section IV with $\alpha = 0.25$ and $r = 1/2$. There are $L = 3$ propagation paths, the window for channel estimation is $rT = 5$ coded symbols, and the normalized Doppler shift $f_D T_s = 0.0093$. The data and channel estimation filters average over the channels of the interferers (Case 2). Simulation results are shown for $N = 128$.

For each code rate and E_b/N_0 , we calculate the PDR that minimizes the probability of error expression as discussed in Section IV. The optimal PDR is used to compute the union bound on coded error probability, and is also the PDR used in the simulation. In contrast to the results with perfect channel estimates, the results for the MMSE filter with pilot-assisted channel estimates show that the rate 1/4 code offers a 1 dB gain relative to the rate 1/2 code uniformly over the range of E_b/N_0 shown. The performance is therefore improved in that case by allocating more degrees of freedom (bandwidth expansion) to error control coding. Again, the rate 1/4 code is best for the MF.

VI. CONCLUSIONS

We have studied the performance of the linear MMSE receiver for DS-CDMA as a function of the PDR and code rate in the presence of frequency-selective fading. A large system analysis has been presented which can be used to optimize the PDR and code rate as a function of load, E_b/N_0 , number of propagation paths, and channel estimation filter length. If the MMSE filter averages over the channels of the interferers, corresponding to an adaptive filtering implementation in moderate to fast fading, then our numerical results show that the optimal PDR for the MMSE receiver is less than that for the MF receiver. If the MMSE receiver incorporates estimates of the channels for all users, then the optimal PDR for the MMSE receiver is greater than that for the MF receiver. For the load and E_s/N_0 considered, a minor performance gain is associated with estimating all of the users' channels, as opposed to the performance associated with the adaptive filtering implementation.

The optimal code rate is generally higher for the MMSE receiver than for the MF receiver, which allows more degrees of freedom for interference suppression. In the presence of frequency-selective fading, the MMSE receiver benefits from using low code rates (again assuming that the MMSE receiver averages over the channels of the interferers). This benefit is enhanced with imperfect channel estimates. Our numerical results for cutoff rate show that in the presence of frequency-selective fading, the performance with the optimal code rate for the MMSE receiver approaches that for the MF, although the MMSE receiver is more robust with respect to the choice of a suboptimal code rate.

APPENDIX
DERIVATION OF (16) AND (23)

Given a matrix \mathbf{A} , we denote the empirical distribution function (e.d.f.) of eigenvalues as $G_{\mathbf{A}}$ which has the Stieltjes transform

$$m_{\mathbf{A}}(z) \equiv \int \frac{1}{\lambda - z} dG_{\mathbf{A}}(\lambda) \quad \text{for } z \in \mathbb{C}^+ \quad (33)$$

where $\mathbb{C}^+ \equiv \{z \in \mathbb{C} : \text{Im}[z] > 0\}$ [16].

Let the $(K-1) \times (K-1)$ matrix $\mathbf{R}_I = \mathbf{B} + \tilde{\mathbf{P}}\tilde{\mathbf{D}}\tilde{\mathbf{P}}^\dagger$ where \mathbf{B} is Hermitian, $\tilde{\mathbf{P}}$ is $N \times (K-1)$ and has i.i.d. elements, $\tilde{\mathbf{D}}$ is $(K-1) \times (K-1)$ and diagonal, and \mathbf{B} , $\tilde{\mathbf{P}}$ and $\tilde{\mathbf{D}}$ are independent. It is shown in [16] that as $N, K \rightarrow \infty$ and $K/N \rightarrow \alpha$, $m_{\mathbf{R}_I}(z)$ converges in distribution to

$$m_{\mathbf{R}_I}(z) = m_{\mathcal{B}} \left(z - \alpha \int \frac{\lambda}{1 + \lambda m_{\mathcal{R}_I}(z)} dG_D(\lambda) \right) \quad (34)$$

where $m_{\mathcal{B}}(z)$ is the limit of the Stieltjes transform of the e.d.f. of \mathbf{B} , and $G_D(\cdot)$ is the asymptotic distribution of the diagonal elements of $\tilde{\mathbf{D}}$.

In [3], it is shown that as $N, K \rightarrow \infty$ and $K/N \rightarrow \alpha$, the SINR at the output of the MMSE filter, γ_{mmse} , converges in probability to

$$\gamma_{mmse}^* = \int_0^\infty \frac{E_1}{\lambda + 2\sigma^2} dG_{\mathcal{R}_I}(\lambda) = E_1 m_{\mathcal{R}_I}(-2\sigma^2) \quad (35)$$

where $G_{\mathcal{R}_I}$ is the limiting eigenvalue distribution of the random interference covariance matrix. Since $m_{\mathcal{R}_I}(z)$ is not defined for real-valued z , and must be in \mathbb{C}^+ , as in [3], we define $m_{\mathcal{R}_I}(-2\sigma^2)$ as the limit of $m_{\mathcal{R}_I}(z)$ as z approaches $-2\sigma^2$ from within \mathbb{C}^+ . Since the elements of $\tilde{\mathbf{P}} = \mathbf{P}_{1-}$ are i.i.d., (34) is used with $\mathbf{B} = \mathbf{0}$ to prove (14).

Orthogonally Multiplexed Pilot

Let $\mathbf{R} = \mathbf{P}\mathbf{D}\mathbf{P}^\dagger + \tilde{\mathbf{P}}\tilde{\mathbf{D}}\tilde{\mathbf{P}}^\dagger + 2\sigma^2\mathbf{I}$ be the covariance matrix of the received signal with an orthogonally multiplexed pilot, where the columns of $\tilde{\mathbf{P}}$ are the pilot spreading sequences and $\tilde{\mathbf{D}} = \beta\mathbf{D}$. We wish to evaluate the large system Stieltjes transform $m_{\mathcal{R}_I}(z)$. In the proof of (34) in [16], the columns of $\tilde{\mathbf{P}}$ are required to be independent so that as $N \rightarrow \infty$,

$$\mathbf{p}_k^\dagger \mathbf{R}^{-1} \mathbf{p}_k \rightarrow \frac{m_{\mathcal{R}_I}(-2\sigma^2)}{1 + A_k^2 E_k m_{\mathcal{R}_I}(-2\sigma^2)}$$

for all k . Here, the k th column of \mathbf{P} is not independent of the k th column of $\tilde{\mathbf{P}}$. However, we show that $\mathbf{p}_k^\dagger \mathbf{R}^{-1} \mathbf{p}_k$ still converges to

$$\frac{m_{\mathcal{R}_I}(-2\sigma^2)}{1 + A_k^2 E_k m_{\mathcal{R}_I}(-2\sigma^2)} \quad \text{as } N \rightarrow \infty.$$

Let $\check{\mathbf{R}}_{k-} = \mathbf{R} - A_k^2 E_k \mathbf{p}_k \mathbf{p}_k^\dagger$ and $\mathbf{R}_{k-} = \check{\mathbf{R}}_{k-} - \check{A}_k^2 E_k \check{\mathbf{p}}_k \check{\mathbf{p}}_k^\dagger$. Applying the matrix inversion lemma gives

$$\mathbf{p}_k^\dagger \mathbf{R}^{-1} \mathbf{p}_k = \frac{\mathbf{p}_k^\dagger \check{\mathbf{R}}_{k-}^{-1} \mathbf{p}_k}{1 + A_k^2 E_k \mathbf{p}_k^\dagger \check{\mathbf{R}}_{k-}^{-1} \mathbf{p}_k} \quad (36)$$

and

$$\mathbf{p}_k^\dagger \check{\mathbf{R}}_{k-}^{-1} \mathbf{p}_k = \mathbf{p}_k^\dagger \mathbf{R}_{k-}^{-1} \mathbf{p}_k - \check{A}_k^2 E_k \frac{\mathbf{p}_k^\dagger \mathbf{R}_{k-}^{-1} \check{\mathbf{p}}_k \check{\mathbf{p}}_k^\dagger \mathbf{R}_{k-}^{-1} \mathbf{p}_k}{1 + \check{A}_k^2 E_k \check{\mathbf{p}}_k^\dagger \mathbf{R}_{k-}^{-1} \check{\mathbf{p}}_k}. \quad (37)$$

We now show that $\mathbf{p}_k^\dagger \mathbf{R}_{k-}^{-1} \check{\mathbf{p}}_k \rightarrow 0$ as $N \rightarrow \infty$, so that $\mathbf{p}_k^\dagger \check{\mathbf{R}}_{k-}^{-1} \mathbf{p}_k \rightarrow m_{\mathcal{R}_I}(-2\sigma^2)$ and

$$\mathbf{p}_k^\dagger \mathbf{R}^{-1} \mathbf{p}_k \rightarrow \frac{m_{\mathcal{R}_I}(-2\sigma^2)}{1 + A_k^2 E_k m_{\mathcal{R}_I}(-2\sigma^2)}$$

as desired.

Let $\mathbf{R}_{k-} = \mathbf{P}_{k-} \mathbf{D}_{k-} \mathbf{P}_{k-}^\dagger + \beta \check{\mathbf{P}}_{k-} \mathbf{D}_{k-} \check{\mathbf{P}}_{k-}^\dagger + 2\sigma^2 \mathbf{I}$ where

$$\mathbf{P}_{k-} = [\mathbf{P}_1, \mathbf{P}_2, \dots, \mathbf{P}_{k-1}, \mathbf{P}_{k+1}, \dots, \mathbf{P}_K] \quad (38)$$

and

$$\check{\mathbf{P}}_{k-} = [\check{\mathbf{P}}_1, \check{\mathbf{P}}_2, \dots, \check{\mathbf{P}}_{k-1}, \check{\mathbf{P}}_{k+1}, \dots, \check{\mathbf{P}}_K]. \quad (39)$$

It will be convenient to write $\mathbf{P}_{k-} = [\mathbf{X}_1^\dagger, \mathbf{X}_2^\dagger]^\dagger$ and $\check{\mathbf{P}}_{k-} = [\mathbf{X}_1^\dagger, -\mathbf{X}_2^\dagger]^\dagger$ where \mathbf{X}_1 and \mathbf{X}_2 have $N/2$ rows. We can then write

$$\begin{aligned} \mathbf{R}_{k-} &= \begin{bmatrix} (1+\beta)\mathbf{X}_1 \mathbf{D}_{k-} \mathbf{X}_1^\dagger + 2\sigma^2 \mathbf{I} & (1-\beta)\mathbf{X}_1 \mathbf{D}_{k-} \mathbf{X}_2^\dagger \\ (1-\beta)\mathbf{X}_2 \mathbf{D}_{k-} \mathbf{X}_1^\dagger & (1+\beta)\mathbf{X}_2 \mathbf{D}_{k-} \mathbf{X}_2^\dagger + 2\sigma^2 \mathbf{I} \end{bmatrix} \\ &= \begin{bmatrix} \mathbf{R}_{1,1} & \mathbf{R}_{1,2} \\ \mathbf{R}_{1,2}^\dagger & \mathbf{R}_{2,2} \end{bmatrix}. \end{aligned} \quad (40)$$

Let $\mathbf{p}_k^\dagger \mathbf{R}_{k-}^{-1} \check{\mathbf{p}}_k = \mathbf{p}_k^\dagger \mathbf{Q} \mathbf{p}_k$ where

$$\mathbf{Q} = \begin{bmatrix} \mathbf{Q}_{1,1} & \mathbf{Q}_{1,2} \\ -\mathbf{Q}_{1,2}^\dagger & \mathbf{Q}_{2,2} \end{bmatrix} = \mathbf{R}_{k-}^{-1} \begin{bmatrix} \mathbf{I} & \mathbf{0} \\ \mathbf{0} & -\mathbf{I} \end{bmatrix} \quad (41)$$

$\mathbf{Q}_{1,1} = (\mathbf{R}_{1,1} - \mathbf{R}_{1,2} \mathbf{R}_{2,2}^{-1} \mathbf{R}_{1,2}^\dagger)^{-1}$, $\mathbf{Q}_{1,2} = \mathbf{Q}_{1,1} \mathbf{R}_{1,2} \mathbf{R}_{2,2}^{-1}$, and $\mathbf{Q}_{2,2} = -(\mathbf{R}_{2,2} - \mathbf{R}_{1,2} \mathbf{R}_{1,1}^{-1} \mathbf{R}_{1,2}^\dagger)^{-1}$. Since \mathbf{p}_k and \mathbf{Q} are independent, the random variable $\mathbf{p}_k^\dagger \mathbf{Q} \mathbf{p}_k$ converges in probability to $(1/N) \text{tr}(\mathbf{Q}) = (1/N) \text{tr}(\mathbf{R}_{1,1} - \mathbf{R}_{1,2} \mathbf{R}_{2,2}^{-1} \mathbf{R}_{1,2}^\dagger)^{-1} - (1/N) \text{tr}(\mathbf{R}_{2,2} - \mathbf{R}_{1,2} \mathbf{R}_{1,1}^{-1} \mathbf{R}_{1,2}^\dagger)^{-1}$ as $N \rightarrow \infty$ [16].

We now show that $\text{tr}(\mathbf{R}_{1,1} - \mathbf{R}_{1,2} \mathbf{R}_{2,2}^{-1} \mathbf{R}_{1,2}^\dagger)^{-1}$ and $\text{tr}(\mathbf{R}_{2,2} - \mathbf{R}_{1,2} \mathbf{R}_{1,1}^{-1} \mathbf{R}_{1,2}^\dagger)^{-1}$ converge to the same deterministic value as $N \rightarrow \infty$. We have

$$\begin{aligned} \mathbf{Q}_{1,1}^{-1} &= \mathbf{R}_{1,1} - \mathbf{R}_{1,2} \mathbf{R}_{2,2}^{-1} \mathbf{R}_{1,2}^\dagger \\ &= \mathbf{X}_1 \left[u \mathbf{D}_{k-} - v^2 \mathbf{D}_{k-} \mathbf{X}_2^\dagger (u \mathbf{X}_2 \mathbf{D}_{k-} \mathbf{X}_2^\dagger + 2\sigma^2 \mathbf{I})^{-1} \right. \\ &\quad \left. \cdot \mathbf{X}_2 \mathbf{D}_{k-} \right] \mathbf{X}_1^\dagger + 2\sigma^2 \mathbf{I} \\ &= \mathbf{X}_1 \left[\frac{u^2 - v^2}{u} \mathbf{D}_{k-} - \frac{2\sigma^2 v^2}{u} \right. \\ &\quad \left. \cdot (\mathbf{X}_2^\dagger \mathbf{X}_2 + 2\sigma^2 \mathbf{D}_{k-}^{-1})^{-1} \right] \mathbf{X}_1^\dagger + 2\sigma^2 \mathbf{I} \end{aligned} \quad (42)$$

where $u = 1 + \beta$, $v = 1 - \beta$ and the last step follows from the matrix inversion lemma. The eigenvalue distribution of $\mathbf{X}_2^\dagger \mathbf{X}_2 + 2\sigma^2 \mathbf{D}_{k-}^{-1}$ converges almost surely as $N \rightarrow \infty$ to a function with Stieltjes transform that is independent of the elements of \mathbf{X}_2 [16]. Consequently, the eigenvalue distribution of $((u^2 - v^2)/u) \mathbf{D}_{k-} - (2\sigma^2 v^2/u) (\mathbf{X}_2^\dagger \mathbf{X}_2 + 2\sigma^2 \mathbf{D}_{k-}^{-1})^{-1}$ converges almost surely as $N \rightarrow \infty$. It follows from [22, Theorem 1.1] that the eigenvalue distribution of $\mathbf{Q}_{1,1}$ converges almost surely to a function which depends only on α, σ^2, β , and the distribution of the diagonal elements of \mathbf{D}_{k-} .

The same arguments show that the eigenvalue distribution of $\mathbf{Q}_{2,2}$ converges to the same function as the system becomes large. Therefore, as $N \rightarrow \infty$ and $K/N \rightarrow \alpha$, $\text{tr}(\mathbf{Q}) \rightarrow 0$ and $\mathbf{p}_k^\dagger \mathbf{R}_{k-}^{-1} \check{\mathbf{p}}_k \rightarrow 0$ in probability. Consequently, we can treat \mathbf{p}_k and $\check{\mathbf{p}}_k$ as though they were independent random vectors and rewrite (34) as

$$m_{\mathcal{R}_I}(z) = \left[-z + \alpha \int \frac{\lambda}{1 + \beta + \lambda m_{\mathcal{R}_I}(z)} + \frac{\beta \lambda}{1 + \beta + \beta \lambda m_{\mathcal{R}_I}(z)} dF_I(\lambda) \right]^{-1}. \quad (43)$$

Combining with (35) gives (16).

Channel Estimation

The signal used for channel estimation (8) can be re-written as

$$\mathbf{r}_T(i) = \sum_{k=1}^K \sum_{l=1}^L h_{k,l} \sqrt{E_k} \mathbf{x}_{T,k}^{(l)}(i) + \mathbf{z}_T(i) + \boldsymbol{\xi}_T(i) \quad (44)$$

where $\mathbf{x}_{T,k}^{(l)}(i) = [\mathbf{x}'_k(i-T+1), \mathbf{x}'_k(i-T+2), \dots, \mathbf{x}'_k(i)]'$ and $\mathbf{z}_T(i)$ and $\boldsymbol{\xi}_T(i)$ are the corresponding AWGN and intersymbol interference. Since consecutive symbols from a given user are independent with mean zero, the interference covariance matrix can be written as

$$\mathbf{R}_I = \begin{bmatrix} \mathbf{B}_1 & \mathbf{0} & \cdots & \mathbf{0} \\ \mathbf{0} & \mathbf{B}_2 & \cdots & \mathbf{0} \\ \vdots & \vdots & \ddots & \vdots \\ \mathbf{0} & \mathbf{0} & \cdots & \mathbf{B}_T \end{bmatrix} \quad (45)$$

where we again neglect the intersymbol interference due to multipath,

$$\mathbf{B}_n = \sum_{l=1}^L \left[\mathbf{P}_{[1,N]}^{(l)} \mathbf{D}_l \left(\mathbf{P}_{[1,N]}^{(l)} \right)^\dagger + \beta \check{\mathbf{P}}_{[1,N]}^{(l)} \mathbf{D}_l \left(\check{\mathbf{P}}_{[1,N]}^{(l)} \right)^\dagger \right] - \frac{\beta E_1}{1+\beta} |h_{1,1}|^2 \check{\mathbf{p}}_1 \check{\mathbf{p}}_1^\dagger \quad (46)$$

$\mathbf{P}_{[1,N]}^{(l)}$ and $\check{\mathbf{P}}_{[1,N]}^{(l)}$ are $N \times K$ matrices whose k th columns contain elements 1 through $N-l+1$ of \mathbf{p}_k and $\check{\mathbf{p}}_k$, respectively, in rows l through N , and \mathbf{D}_l is a diagonal matrix with k th entry given by $E_k |h_{k,l}|^2 / (1+\beta)$.

As $N \rightarrow \infty$ and $K/N \rightarrow \alpha$ the Stieltjes transform of \mathbf{B}_n converges to

$$m_{\mathbf{B}}(z) = \left[-z + \alpha \int \frac{\lambda}{1 + \lambda m_{\mathbf{B}}(z)} dF_I(\lambda) \right]^{-1} \quad (47)$$

which is independent of n . The effects of the pilot and data signals are accounted for in $F_I(\cdot)$. From (45) the set of eigenvalues of \mathbf{R}_I is equal to the union of the T sets of eigenvalues of \mathbf{B}_n , $1 \leq n \leq T$. Therefore the e.d.f. of \mathbf{R}_I is the scaled sum of the component e.d.f.s, $G_{\mathbf{R}_I} = \sum_{n=1}^T (1/T) G_{\mathbf{B}_n}$. Substituting into (33) gives $m_{\mathbf{R}_I}(z) = \sum_{n=1}^T (1/T) m_{\mathbf{B}_n}(z)$ and taking the limit of both sides as $N \rightarrow \infty$, we obtain $m_{\mathbf{R}_I}(z) = \sum_{n=1}^T (1/T) m_{\mathbf{B}}(z) = m_{\mathbf{B}}(z)$. Combining this with (35) and noting that the desired average signal energy per path is $(\beta/(1+\beta))TE_1/L$ gives (23).

Note that (47) is the same as the analogous limit for a multicode system in which each user transmits T independent spreading sequences, each of length NT , and with power scaled by $1/T$. This approach can be extended to a multirate system model using variable spreading factors [23]. An alternative proof of (47) in this latter scenario is presented in [14] using results from [15]. However, the proof presented here is simpler and more direct than that used to prove the corollary cited in [15].

ACKNOWLEDGMENT

The authors thank Dr. B. Vojcic for first suggesting the use of cutoff rate to optimize the code rate and the editor and anonymous reviewers for their detailed comments which helped to improve the paper.

REFERENCES

- [1] European Telecommunications Standards Institute, "The ETSI UMTS Terrestrial Radio Access (UTRA) ITU-R RTT Candidate Submission," 1998.
- [2] P. Chaudhury, W. Mohr, and S. Onoe, "The 3GPP proposal for IMT-2000," *IEEE Commun. Mag.*, pp. 72–81, Dec. 1999.
- [3] D. N. C. Tse and S. V. Hanly, "Linear multiuser receivers: Effective interference, effective bandwidth and user capacity," *IEEE Trans. Inform. Theory*, pp. 641–657, Mar. 1999.
- [4] J. Evans and D. N. C. Tse, "Large system performance of linear multiuser receivers in multipath fading channels," *IEEE Trans. Inform. Theory*, pp. 2059–2078, Sept. 2000.
- [5] S. L. Miller, M. L. Honig, and L. B. Milstein, "Performance analysis of MMSE receivers for DS-CDMA in frequency-selective fading," *IEEE Trans. Commun.*, pp. 1919–1929, Nov. 2000.
- [6] P. Schramm, "Analysis and optimization of pilot-channel-assisted BPSK for DS-CDMA systems," *IEEE Trans. Commun.*, pp. 1122–1124, Sept. 1998.
- [7] F. Ling, "Optimal reception, performance bound and cut-off rate analysis of reference-assisted coherent CDMA communications with applications," *IEEE Trans. Commun.*, pp. 1583–1592, Oct. 1999.
- [8] V. Veeravalli and B. Aazhang, "On the coding-spreading tradeoff in CDMA systems," in *Proc. 1996 Conf. Inform. Sci. Syst.* '96, Mar. 1996, pp. 1136–1141.
- [9] M. L. Honig and B. R. Vojcic, "Combined coding and interference suppression for DS-CDMA," in *1998 IEEE Inform. Theory Workshop*, Feb. 1998.
- [10] W. G. Phoel, M. L. Honig, and B. R. Vojcic, "Coded performance of MMSE receivers for DS-CDMA in the presence of fading," in *Proc. 1999 Conf. Inform. Sci. Syst.*, Mar. 1999, pp. 249–254.
- [11] J. R. Foerster and L. B. Milstein, "Coding for a coherent DS-CDMA system employing an MMSE receiver in a Rayleigh fading channel," *IEEE Trans. Commun.*, pp. 1012–1021, June 2000.
- [12] E. Biglieri, G. Caire, G. Taricco, and E. Viterbo, "CDMA design through asymptotic analysis: Fading channels," in *Proc. Allerton Conf.*, Sept. 1999.
- [13] V. Veeravalli, "The coding-spreading tradeoff in CDMA systems," in *Proc. Allerton Conf.*, Sept. 1999.
- [14] E. Biglieri, G. Caire, and G. Taricco, "CDMA system design through asymptotic analysis," *IEEE Trans. Commun.*, pp. 1882–1895, Nov. 2000.
- [15] G. Kiran and D. N. C. Tse, "Effective interference and effective bandwidth of linear multiuser receivers in asynchronous CDMA systems," *IEEE Trans. Inform. Theory*, pp. 1426–1447, July 2000.
- [16] J. Silverstein and Z. D. Bai, "On the empirical distribution of eigenvalues of a class of large dimensional random matrices," *J. Multivar. Anal.*, vol. 54, no. 2, pp. 175–192, 1995.
- [17] H. V. Poor and S. Verdú, "Probability of error in MMSE multiuser detection," *IEEE Trans. Inform. Theory*, pp. 858–871, May 1997.
- [18] J. G. Proakis, *Digital Communications*, 3rd ed. New York: McGraw-Hill, Inc., 1995.
- [19] J. Y. N. Hui, "Throughput analysis for code-division multiple accessing of the spread spectrum channel," *IEEE J. Select. Areas Commun.*, pp. 482–486, July 1984.
- [20] J. Zhang, E. K. P. Chong, and D. N. C. Tse, "Output MAI distributions of linear MMSE multiuser receivers in DS-CDMA systems," *IEEE Trans. Inform. Theory*, pp. 1128–1144, Mar. 2001.
- [21] S. Verdú and S. Shamai (Shitz), "Spectral efficiency of CDMA with random spreading," *IEEE Trans. Inform. Theory*, pp. 622–640, Mar. 1999.
- [22] J. Silverstein, "Strong convergence of the empirical distribution of eigenvalues of large dimensional random matrices," *J. Multivar. Anal.*, vol. 55, no. 2, pp. 331–339, 1995.
- [23] W. G. Phoel, "Interference suppression for DS-CDMA with space and time diversity," Ph.D. dissertation, Northwestern Univ., Evanston, IL, June 2000.



Wayne G. Phoel (S'92–M'00) received the B.S. and M.Eng. degrees in electrical engineering from Cornell University, Ithaca, NY, in 1993 and 1994, respectively, and the Ph.D. degree in electrical and computer engineering from Northwestern University, Evanston, IL, in 2000.

From 1994 through 1996, he worked on signal processing for radar applications at Calspan Corporation, Buffalo, NY. He contributed regularly to work at Motorola Cellular Infrastructure Group between 1997 and 2000. Since 2000, he has been a member of the technical staff at the Massachusetts Institute of Technology's Lincoln Laboratory, Lexington. His current research interests are in the areas of communications and information theory with emphasis on modulation and coding.



Michael L. Honig (S'80–M'81–SM'92–F'97) received the B.S. degree in electrical engineering from Stanford University, Stanford, CA, in 1977, and the M.S. and Ph.D. degrees in electrical engineering from the University of California, Berkeley, in 1978 and 1981, respectively.

He subsequently joined Bell Laboratories, Holmdel, NJ, where he worked on local area networks and voiceband data transmission. In 1983, he joined the Systems Principles Research Division at Bellcore, where he worked on digital subscriber lines and wireless communications. He was a visiting lecturer at Princeton University, Princeton, NJ, during fall 1993. Since fall 1994, he has been with Northwestern University, Evanston, IL, where he is a Professor with the Electrical and Computer Engineering Department.

Dr. Honig was an Editor for the IEEE TRANSACTIONS ON INFORMATION THEORY and the IEEE TRANSACTIONS ON COMMUNICATIONS, and was a Guest Editor for the *European Transactions on Telecommunications* and *Wireless Personal Communications*. He was also a member of the Digital Signal Processing Technical Committee for the IEEE Signal Processing Society. He is a member of the Board of Governors for the Information Theory Society.